Journal of Microscopy, Vol. 202, Pt 2, May 2001, pp. 374–378.
Received 28 August 2000; accepted 11 October 2000

Near-field effects in single molecule emission

H. GERSEN*, M. F. GARCÍA-PARAJÓ*, L. NOVOTNY†, J. A. VEERMAN*, L. KUIPERS AND N. F. VAN HULST*

**Applied Optics Group, Department of Applied Physics and MESA+ Research Institute, University of Twente, PO Box 217, 7500 AE Enschede, The Netherlands*
†The Institute of Optics, University of Rochester, Rochester, NY 14627, U.S.A.

Key words. 3D orientation determination, absorption and emission dipole moment, edge and boundary effects, fluorescence microscopy, near-field scanning optical microscopy, polarization microscopy, single molecule detection

Summary

We present the first experimental proof of the influence of a nearby nano-sized metal object on the angular photon emission by a single molecule. A novel angular sensitive detection scheme is implemented in an existing near-field scanning optical microscope (NSOM). The positioning accuracy (~1 nm) of the NSOM allows a systematic investigation of the intensity ratio between two different half-spaces as a function of the position of the metal–glass interfaces of the probe with respect to the single emitter. The observed effects are shown to be particularly strong for molecules that are excited mainly below the rims of the aperture. An excellent agreement is found between experiments and numerical simulations for these molecules. The observed angular redistribution of the angular emission of a single molecule could explain the alteration of the emission polarization observed for certain molecules in earlier experiments (Veerman *et al.* (1999) *J. Microsc.* **194**, 477–482).

Introduction

Among the exciting possibilities opened up by the advances in room-temperature single molecule detection is the prospect of obtaining a complete understanding of complex molecular systems. As a single fluorescent molecule can be viewed as a local reporter of its nano-environment, it can be exploited in a way not possible in an ensemble study. By interrogation of the transition dipole moment of a rigidly attached probe by polarized excitation/emission, direct detection of the three-dimensional (3D) orientation of the components of a macro-molecule relative both to each other, and to nearby interfaces becomes possible. As a change in the local environment influences the (molecular) properties it is essential to understand the electromagnetic interaction with nearby objects to determine the 3D orientation. The exact determination of the molecular 3D orientation is of vital importance in fluorescence resonance energy transfer experiments (Ha *et al.*, 1996) and in the study of time-dependent phenomena such as protein and molecular conformational changes.

The 3D orientation of individual absorption dipole moments can be determined in excitation using near-field scanning optical microscopy (NSOM) as a result of the field emanating from the NSOM-probe (Betzig & Chichester, 1993). The individual molecules were immobilized on a planar substrate and locally excited with a metal-coated light emitting probe that was scanned in close proximity to the sample surface. By controlling the polarization of the excitation light the authors determined the absorption dipole orientation for each molecule in three dimensions. Extending the NSOM with a polarization sensitive detection scheme allows the in-plane emission dipole moment to be determined. This is achieved by monitoring the relative contribution of the fluorescence signal in two perpendicular polarized directions (Ruiter *et al.*, 1997). However, the polarization of the emission does not provide unique values for the in-plane emission dipole moment, as the detected signal contains an unpolarized contribution from the emission dipole component along the optical axis. However, the full 3D orientation of the emission dipole can be properly extracted if the molecular emission pattern is taken into account. Thus, a detailed analysis of the molecular excitation/emission polarization patterns allows quantitative 3D determination of both the molecular absorption and emission dipole orientation.

Obviously, for a fixed orientation of the emission dipole a fixed polarization of the emission is expected. In our measurements, however, we have observed many molecules that exhibit an apparent alteration of the emission

Correspondence to: H. Gersen. Tel: + 31 53 489 4002; fax: + 31 53 489 1105; e-mail: h.gersen@tn.utwente.nl

polarization that depends on the position of the molecule with respect to the near-field probe (Veerman *et al.*, 1999). The molecules are immobilized in a thin polymethylmethacrylate (PMMA) layer. Rotational diffusion and reorientation of the immobilized molecules therefore only occurs for small numbers of molecules and can be directly visualized (Ruiter *et al.*, 1997). As the molecules are stationary in time the question arises whether a change in the angular emission of the molecule could be the origin of the observed effect. A change in the angular emission can be directly coupled to an overall detected polarization change as it changes the angles at which the light enters the objective. This is because a high NA objective influences the polarization as polarization components of light entering the objective at high angles are partly projected onto the orthogonal polarization direction, which causes a reduction of the measured polarization ratio (Axelrod, 1979).

In this paper, we present the first experimental proof for the redirection of the angular emission of an individual molecule as induced by the close proximity of the NSOM probe. Using a novel angular sensitive detection scheme, we directly quantify the degree of angular emission pattern modification for molecules with a dipole moment oriented along the optical axis as the probe is scanned laterally along the sample surface. The observed effect is compared with calculations based on the multiple multipole (MMP) technique and could explain the observed alterations of the emission polarization within the excitation pattern of a single molecule.

To investigate the effect of the near-field probe on the single molecule emission pattern it is essential to detect the fluorescence emission as a function of the emission angle. For this purpose we implemented a new experimental scheme exploiting the fact that the fluorescence emitted by the molecule at a given angle in the focus of an objective emerges at a well-defined position in a plane behind the objective. A specific area of this plane is directed to a detector, giving information concerning the emission at angles corresponding to that area. To obtain maximum sensitivity for asymmetric emission, and still have sufficient photons to allow single molecule detection, we separate the emission at the optical axis in two different parts given by the $-x$ and $+x$ half-space (see Fig. 1). Each of these half-spaces is focused on a separate photon-counting avalanche photo diode (APD). This new detector configuration (Fig. 1) has been implemented in an existing NSOM set-up described in detail elsewhere (Ruiter *et al.*, 1997). In this way, a detection scheme is realized with a signal ratio between two detectors that is sensitive for both a probe-induced modification of the angular emission and for the relative contribution of a stationary emission in the two half spaces.

The separation in two different half-spaces is accomplished by inserting a reflecting knife-edge parallel to the y-axis. The insertion of a knife-edge along the y-axis results in a method exclusively sensitive for asymmetries in the x-z plane (z is the optical axis). Asymmetry in the y-z plane obviously requires separation of the signal along the x-direction. In both cases the same information is obtained, yet for a different set of fluorescent molecules. The reflection layer on the knife-edge is made by evaporating a thin layer of silver on a microscope cover-slide (76 × 23 mm, cut edges) resulting in a reflection coefficient of 98.0 ± 0.5% and 94 ± 1% for s- and p-polarization, respectively. We use the excitation light emitted by the NSOM probe to align the experimental set-up. Subsequently, the angular emission can be split in two equal parts with an accuracy of better then 1.5% as determined from the background signal on the two detectors. This background mainly originates from the luminescence of the fibre.

For the experiment itself, we bring an aluminium coated tapered optical fibre in close proximity to individual molecules. The near-field optical probes in our experiment are modified by side-on milling with a focused ion beam (FIB) (Veerman *et al.*, 1998). We obtain probes with a flat end-face (surface roughness < 1.5 nm) and a well-defined circular aperture with a radius of ~80 nm (Veerman *et al.*, 1999). The higher the sharpness of the rims of the aperture, the higher the gradients of the optical field and the more pronounced the near-field effects. For the optical field the edge sharpness of the metal–glass interface is solely determined by the optical penetration depth of the metal (6 nm for Al.).

Figure 2 shows a set of angle specific single molecule images in which a false-colour scale is applied that represents the relative contribution of the two half-spaces to the collected power. Red and green are used to indicate the power emitted to the half-spaces given by the negative and positive x-directions, respectively. An equal signal on both detectors results in a yellow colour. In Fig. 2(a) a typical

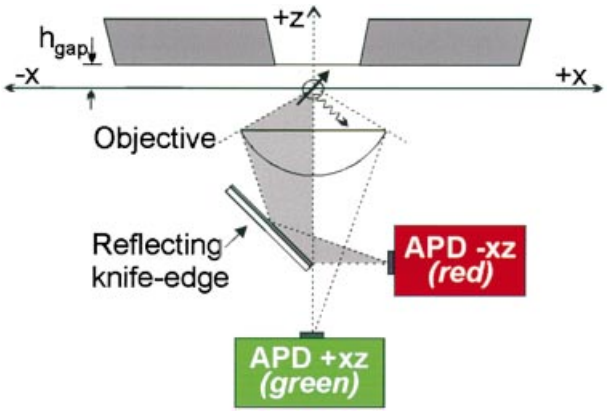

Fig. 1. Detection scheme for angle specific detection. Fluorescence emitted at a given solid angle corresponds to a specific area in a plane behind the objective. The knife-edge in that plane, placed parallel to the y-axis (out of paper), separates the emission in the $-x$ and $+x$ half-spaces.

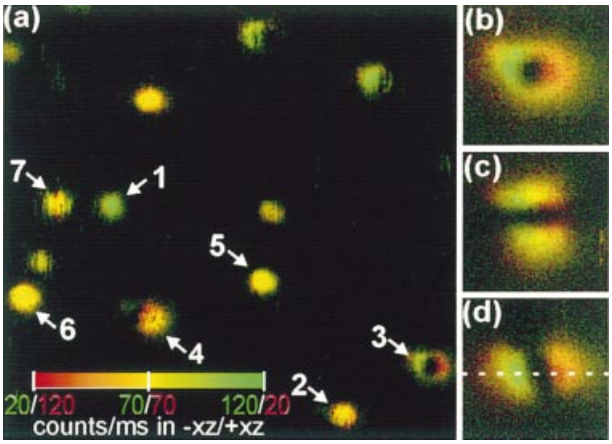

Fig. 2. Angle specific NSOM fluorescence images obtained with an ~80 nm aperture probe showing $DiIC_{18}$ molecules embedded in a 10-nm thin film of PMMA (10^{-9} M) with a probe–sample separation of 20 ± 5 nm (scan-direction along *y*). The false-colour scale (red/green) indicates emission contribution into the $-x$ and $+x$ half-spaces, respectively. An equal signal on both detectors results in a yellow colour.(a) Scan 2.6×2.6 μm^2, circular polarized excitation. (b)–(d) Detailed scans (450×450 nm^2) of a molecule oriented along the optical axis with, respectively, circular, and linear *y*- and *x*-polarized excitation light. For (b)–(d) the same colour-scale as given in (a) applies, yet the counts in the two half-spaces now range from 3 to 30 counts/ms.

measurement (2.6×2.6 μm^2) for circularly polarized excitation light is shown. Several important observations can be made. Firstly, the observed near-field excitation patterns correspond well to the expected intensity patterns of the Bethe–Bouwkamp model (Bethe, 1944; Bouwkamp, 1950; Betzig & Chichester, 1993; Veerman *et al.*, 1999) generated by the overlap of the molecular absorption dipole moment with the electrical fields present close to the aperture. This overlap means that a molecule undergoes selective excitation as a function of its position with respect to the probe and its dipole orientation. The in-plane molecules are preferentially excited when they are centred beneath the near-field probe while the *z*-oriented molecules are excited mainly close to the aperture rims. In the latter case, for example, the molecular excitation patterns show up as rings when circularly polarized excitation light is used. From the lateral dimensions of the excitation patterns the probe–sample separation is estimated to be 20 ± 5 nm. Secondly, overall 'colour' differences between different molecules can be distinguished as can be clearly seen by comparing for example, molecules 1 and 2. This asymmetric distribution of the total amount of photons emitted by a molecule between the $-x$ and $+x$ half space indicates an out-of-plane component of the emission dipole. For molecules with given fixed emission dipole orientation a fixed asymmetry (and thus colour) is therefore expected.

However, one can clearly observe 'colour' variations within the near-field excitation pattern, e.g. molecules 3 and 4. These 'colour' variations indicate a redistribution of the emitted photons over the two half-spaces as the probe is scanned over the molecule. Any influence of the probe on the molecular emission is expected to be strongly dependent on the position of the probe with respect to the molecule. Therefore, we attribute the observed redistribution of radiation to the presence of the metal-glass transitions of the probe. The observed effects are particularly strong for molecules with a significant *z*-component, e.g. molecules 3 and 4, whereas for molecules 5 and 6 with mainly an in-plane orientation the effect is less pronounced.

Figures 2(b–d) display detailed scans on a z-orientated molecule (450×450 nm^2) at a probe-sample separation of 20 ± 5 nm for circularly and linearly *y*- and *x*-polarized excitation light ($\lambda = 514$ nm), respectively. The molecular orientation is determined directly from the excitation pattern and the fact that the total amount of photons emitted between the $-x$ and $+x$ half-spaces has to be symmetric. Both criteria are relevant as absorption and emission polarization characteristics should be taken into account separately as an angle between emission and adsorption dipole moment can be present. In Fig. 3(a) a cross-section through the excitation pattern of the *z*-oriented molecule taken at the dashed line in Fig. 2(d) is presented. The *z*-oriented molecule is preferentially excited below the rims as a result of the strong *z*-component of the

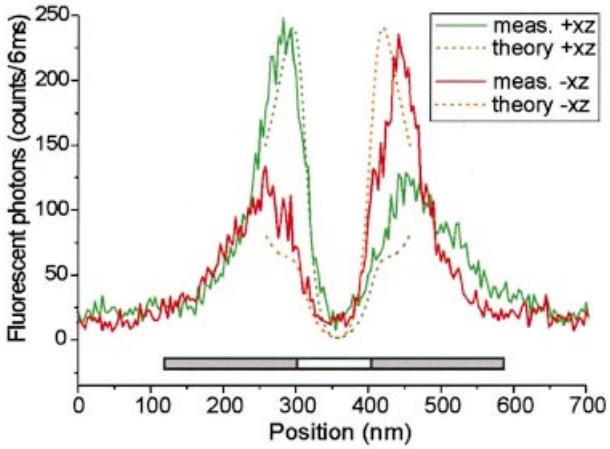

Fig. 3. The fluorescence of both half-spaces displayed separately (solid curves) for a *z*-oriented molecule in Fig. 2(d) (at dashed line). Six adjacent scan-lines have been added. Here the excitation is *x*-polarized. Maximum excitation of this molecule occurs at the gradient field around the metal–glass transitions. Clearly between two to three times more signal is collected in one half-space with respect to the other half-space below the aperture rims. The dotted curves present the result of the numerical simulation for the experimental geometry depicted in Fig. 1 (parameters given in text). An excellent agreement between theory and experiment is observed. The inset shows the dimensions of the probe compared to the measured excitation pattern.

excitation field there, giving rise to the double lobe structure. To display the asymmetry between the two half-spaces the cross-section has to be taken perpendicular to the knife-edge and not along the polarization-direction of the excitation-light in Fig. 2(d). The excitation pattern only indicates the overlap between absorption-dipole and the electric field of the aperture. Changing the excitation polarization from circular (Fig. 2b) to linear along y and x (Figs 2c and d) therefore only changes the excitation pattern and not the observed asymmetry of the emission. Figure 3 shows that when the molecule is right beneath the aperture rim, one detector detects between two to three times more photons than the other detector. The observed asymmetry as induced by the probe is much larger than the observed asymmetry resulting from a component of the molecular transition dipole along the optical axis. As the observed asymmetric emission is reproducible, we can also exclude the possibility of an emission-dipole reorientation as a function of the lateral position of the probe. It is possible to observe some rotational dynamics, e.g. molecule 7 in Fig. 2(a). For this molecule we observe discrete jumps between different z-components. Molecules with such a dynamic behaviour have been excluded from our analysis.

In our experiment, the scan movement of the sample stage is such that the images can be viewed as if the probe is moving across the sample while scanning. Figure 4 schematically depicts the relative probe position and the corresponding direction of the probe-induced effect on the emission pattern for a z-oriented molecule. The sequence (a)–(e) corresponds to a movement of the probe from $-x$ to $+x$. Although the z-oriented molecule in Fig. 4(a) is weakly excited, it can be determined that the fluorescence emission is directed towards the $-x$ half-space (more 'red', Fig. 4a). As the near-field probe scans further, the molecule is strongly excited at the metal–glass interface on the $+x$ side of the probe (Fig. 4b). Now a redirection of the fluorescence towards the $+x$ half-space (more 'green', Fig. 4b) is observed. When the molecule is centred beneath the probe (Fig. 4c) essentially no emission is observed. As the scan continues, the redirection of the angular emission is repeated in reverse (Fig. 4d, e). Thus, it can be concluded that the fluorescence photons of a z-oriented molecule are deflected towards the centre of the aluminium coating as can be derived from comparison with the probe-dimensions (see inset Fig. 3).

To confront the observations with theory, calculations based on the multiple multipole (MMP) technique have been carried out for the 2D geometry depicted in Fig. 1. In these calculations the molecule is modelled as a classical dipole (Drexhage, 1974; Chance *et al.*, 1978; Novotny, 1997). We assume that no angle is present between the absorption- and emission-dipole moment of the molecule so that the molecule is represented by a single dipole orientation. Figure 5 illustrates the angular emission for a dipole oriented along the optical axis on top of an infinite glass substrate ($\varepsilon_{\text{glass}} = 2.5$), both without (Fig. 5a) and with (Fig. 5b) a metal object ($\varepsilon_{\text{aluminium}} = -34.5 + i8.5$) present (Novotny, 1996). Figure 5(b) clearly shows that the angular emission is deflected towards the centre of the metal object when the dipole is below the edges, which is in agreement with our experimental observations. For a direct comparison between calculation and experiment the emission of the emission-dipole is evaluated in both half-spaces as a function of the relative dipole-probe position. In this calculation we use parameters comparable to the experiment (NA = 1.3, $h_{\text{gap}} = 20$ nm, aperture = 100 nm, coating-thickness = 100 nm and emission wavelength = 633 nm). In order to calculate this position dependent

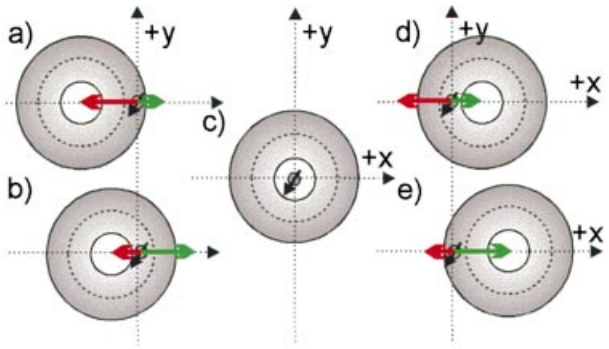

Fig. 4. Schematic illustration of the relative position of the probe during the scan for a z-oriented dipole. Sequence (a)–(e) corresponds to a tip-movement from $-x$ to $+x$. Length of the depicted arrows indicates the relative amount of power emitted into each half-space. A larger relative contribution in the $-x$ and $+x$ half-space corresponds to 'red' and 'green' in Figs 2 and 3, respectively. For a z-oriented molecule the emitted photons are deflected towards the centre of the metal coating.

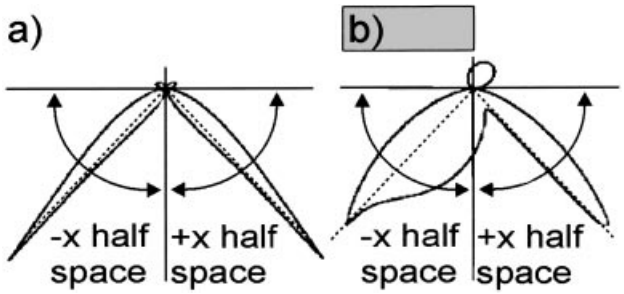

Fig. 5. Illustration of the angular emission of an emitting perpendicular orientated dipole. The dipole is located 1 nm above a planar glass substrate ($\varepsilon = 2.5$). An aluminium object ($\varepsilon = -34.5 + i8.5$) is scanned at a distance of 40 nm above the glass. On the left side no object is present, while on the right side the dipole is located below the rim of the metal object. The emitted photons are deflected towards the metal object. The dashed line indicates the angle of total internal reflection.

angular emission, the excitation field of the near-field probe is included without considering fluorescence quenching. The latter suppresses the emission when the molecule is located beneath the metal coating and therefore only influences the 'apparent' excitation-pattern. The result of this calculation, depicted in Fig. 3, shows an excellent agreement between theory and experiment for *z*-oriented dipoles without any fit to the experimental data.

In summary, for the first time we have observed near-field effects on the emission patterns of single molecules. Due to the close proximity of sharp well-defined material boundaries of FIB modified NSOM probes the angular emission of a single molecule is strongly modified. For *z*-oriented molecules that are excited near the aperture rims the emitted photons are deflected towards the centre of the metal coating in agreement with MMP calculations. The observed modification of the angular emission could explain the observed anomalous alteration of the emission polarization as a function of the relative molecule-probe position observed in earlier experiments.

The strength of the observed effect on the angular emission has severe implications for current efforts to obtain near-field optical imaging based on local field enhancement by sharp metal tips (Sánchez *et al.*, 1999) and the determination of the 3D orientation of emitters in a heterogeneous environment. Furthermore, the experimental configuration as used in this experiment could be useful to determine the full 3D orientation of the emission dipole in an alternative way.

References

Axelrod, D. (1979) Carbocyanine dye orientation in red cell membrane studied by microscopic fluorescence polarization. *Biophys. J.* **26**, 557–573.

Bethe, H.A. (1944) Theory of diffraction by small holes. *Phys. Rev.* **66**, 163–182.

Betzig, E. & Chichester, R.J. (1993) Single molecules observed by near-field scanning optical microscopy. *Science*, **262**, 1422–1425.

Bouwkamp, C.J. (1950) On Bethe's theory of diffraction by small holes. *Philips Res. Report*, **5**, 321–332.

Chance, R.R., Prock, A. & Silbey, R. (1978) Molecular fluorescence and energy transfer near interfaces. *Adv. Chem. Phys.* **37**, 1–65.

Drexhage, K.H. (1974) Interaction of light with monomolecular dye layers. *Prog. Opt.* **12**, 163–232.

Ha, T., Enderle, Th., Ogletree, D.F., Chemla, D.S., Selvin, P.R. & Weiss, S. (1996) Probing the interaction between two single molecules: fluorescence resonance energy transfer between a single donor and a single acceptor. *Proc. Natl. Acad. Sci. U.S.A.* **93**, 6264–6268.

Novotny, L. (1996) Single molecule fluorescence in inhomogeneous environments. *Appl. Phys. Lett.* **69**, 3806–3808.

Novotny, L. (1997) Allowed and forbidden light in near-field optics. I. A single dipolar light source. *J. Opt. Soc. Am.* **14**, 91–104.

Ruiter, A.G.T., Veerman, J.A., García-Parajó, M.F., Van Hulst, N.F. (1997) Single molecule rotational and translational diffusion observed by near-field scanning optical microscopy. *J. Phys. Chem. A.* **101**, 7318–7323.

Sánchez, E., Novotny, L. & Xie, X.S. (1999) Near-field fluorescence microscopy based on two-photon excitation with metal tips. *Phys. Rev. Lett.* **82**, 4014–4017.

Veerman, J.A., García-Parajó, M.F., Kuipers, L., van Hulst, N.F. (1999) Single molecule mapping of the optical field distribution of probes for near-field microscopy. *J. Microsc.* **194**, 477–482.

Veerman, J.A., Otter, A.M., Kuipers, L. & van Hulst, N.F. (1998) High definition aperture probes for near-field optical microscopy fabricated by focused ion beam milling. *Appl. Phys. Lett.* **72**, 3115–3117.